Accepted Manuscript

High-sensitive surface plasmon resonance microRNA biosensor based on streptavidin functionalized gold nanorods-assisted signal amplification

Kaihong Hao, Yu He, Huiting Lu, Shaotao Pu, Yingnan Zhang, Haifeng Dong, Xueji Zhang

PII: S0003-2670(16)31446-5

DOI: 10.1016/j.aca.2016.12.006

Reference: ACA 234950

To appear in: *Analytica Chimica Acta*

Received Date: 9 October 2016

Revised Date: 28 November 2016

Accepted Date: 1 December 2016

Please cite this article as: K. Hao, Y. He, H. Lu, S. Pu, Y. Zhang, H. Dong, X. Zhang, High-sensitive surface plasmon resonance microRNA biosensor based on streptavidin functionalized gold nanorods-assisted signal amplification, *Analytica Chimica Acta* (2017), doi: 10.1016/j.aca.2016.12.006.

High-sensitive surface plasmon resonance microRNA biosensor based on streptavidin functionalized gold nanorods-assisted signal amplification

Kaihong Hao,[a#] Yu He ,[a#] Huiting Lu,[b] Shaotao Pu,[a] Yingnan Zhang,[a] Haifeng Dong,[a] Xueji Zhang[a*]*

[a]*Research Center for Bioengineering and Sensing Technology, School of Chemistry and Bioengineering, University of Science & Technology Beijing, Beijing 100083, P.R.China*

[b]*School of Space and Environment, Beihang University, Beijing 100191, P. R. China*

[a#]*First author contribute to the paper equally.*

ABSTRACT

Herein, a facile and sensitive microRNA (miRNA) biosensor was designed by using interfacial biotinylated thiolated DNA molecular beacon (MB) as probe and streptavidin functionalized gold nanorods (Stre-GNRs) as tag for the enhanced surface plasmon resonance (SPR) signal. The MB probe with two terminals labeled with biotin and thiol groups, respectively, was modified on the gold film via thiol-gold interaction. Up hybridization with the target, the biotinylated group became accessible to the Stre-GNRs. The introduction of the Stre-GNRs tag to the gold film produced strong SPR signal for detection. Our work has illustrated that the plasmonic field extension generated from the gold film to GNRs and the mass increase due to the GNRs have led to drastic sensitivity enhancement. Under optimal conditions, this proposed approach allowed detection of miRNA with the limit of detection (LOD) down to 0.045 pM. The results have shown that the MB probe functionalized sensing film, together with streptavidin-conjugated GNRs, was readily served as a plasmonic coupling partner that can be used as a powerful ultrasensitive sandwich assay for miRNA detection, and GNRs were readily served as promising amplification labels in SPR sensing technology.

Key words: MicroRNA detection; streptavidinylated gold nanorods; surface plasmon resonance (SPR); signal amplification

1. Introduction

MicroRNA (abbreviated miRNA) is a group of endogenous small single-stranded non-coding RNA that functions in RNA silencing and post-transcriptional regulation of gene expression to modulate biological homeostasis [1-3], which is widely found in plants, animals and some viruses [4]. To date, there is growing evidence that miRNAs play crucial roles in various physiological and pathologic processes, including hematopoietic differentiation, cell growth, apoptosis [5, 6], regulation and metabolism, especially the aberrant expression is associated with various tumorigenesis [7-9]. Therefore, development of sensitive and specific analytical methods for miRNAs will be of great value in disease diagnosis, treatment and prognosis [5, 10]. Meantime, it can also make contribution to understand biological functions of miRNAs and discover new targets for drugs [11]. However, the accurate detection of miRNA is challenging because of some intrinsic characteristics of miRNA such as low level in the cell, short sequence and lack of common characteristics [12]. Traditionally, the miRNA detection methods include: Northern blotting [13], microarray chip and quantitative reverse transcription polymerase chain reaction [14, 15], etc. However, they are usually time-consuming, costly, and require highly trained technicians [4, 16], which have intrigued recent development of simple and new signal amplification strategies for miRNA detection [17, 19].

Surface plasmon resonance (SPR) spectroscopy is a wide-used surface analysis method based on changes in the optical reflectivity of a thin metal film (typically gold)

when species adsorb or bind to its surface or to any material coated onto its surface [20, 21]. It has been emerging as an important sensing technique due to the high sensitivity of real-time monitoring and analysis [22]. Specifically, it detects refractive index change caused by any surface coating or solution near the SPR-active metal surface with high sensitivity and fast time resolution [23, 24]. Functionalization of the metal surface with specific binding sites with bioaffinity creates a biosensor that can detect biomolecular interactions in real time with no labeling requirements [23-25]. Therefore, SPR spectroscopy has become a useful tool in biochemistry and bioanalytical chemistry, especially for determining the equilibrium binding constants describing the interactions between proteins, DNAs or RNAs and a wide variety of other biomolecules or ligands, or for investigating the effects of various cofactors or inhibitors on these binding constants [26, 27]. However, the limit of detection (LOD) of a typical SPR biosensor for small molecules based on nonspecific adsorption is at nanomolar level, which has restricted its widespread applications. A variety of approaches have being continuously explored to further enhance the SPR response [28, 29].

Improvement of SPR LOD can be realized by various strategies. Nanoparticles with controlled size, shape, and surface chemistry provide a wide range of new opportunities for designing good performance biosensor. When nanoparticle combine with SPR biosensor, reagents can be conjugated various nanoparticles, especially gold nanoparticles (GNPs) [30-32] and magnetic nanoparticles [20, 33], that increase their mass and refractive index to accomplish improved detectability. Their own SPR

properties (LSPR, localized Surface Plasmon Resonance) of GNPs have also been explored to reinforce the signal by means of electronic coupling of surface and the NP plasmons [34-36]. It was reported that the shape, size and nanogold probes composition influenced the performance of the SPR response [34]. In term of the similar properties to GNPs, gold nanorods (GNRs) possessing flexibility for functionalization, good strong SPR properties and large absorption cross section enables to improve the detectability of SPR response, which has been little explored.

As proof-of-principle, herein, a novel SPR detection strategy by applying biotinylated thiolated molecular beacon (MB) interfacial gene probes and strepavidinylated GNRs (Stre-GNRs) for the enhanced SPR response to realize rapid and sensitive miRNA detection is demonstrated (**Scheme 1**). Briefly, MB gene probes were immobilized on the gold film via thiol-Au interaction, in which the Stre-GNR detection probes were blocked for the interaction with the immobilized biotin end due to the large steric effect. After hybridization with target miRNA, the loop sequence formed a rigid duplex with the target, which broke the relatively shorter stem duplex and ‘‘activated’’ the biotin terminal from the film surface for readily accessibility to the Stre-GNR detection probes. The introduction of detection probe to a sensor surface led to a significantly amplified SPR signal. It is reported that the DNA helix structure is rigid enough for holding up the latex large to 500 nm for signal amplification [37.38]. Thus, we think it is strong enough for holding up the Stre-GNRs (~42 nm) signal tag in this system. It has demonstrated that the plasmonic field extension generating from the gold film to GNRs and the mass increase of the

reagent due to the GNR has led to a drastic sensitivity enhancement. The results have shown that GNRs were readily served as promising amplification labels in SPR sensing technology and were able to provide a broad space for the development of the next generation SPR biosensor technology.

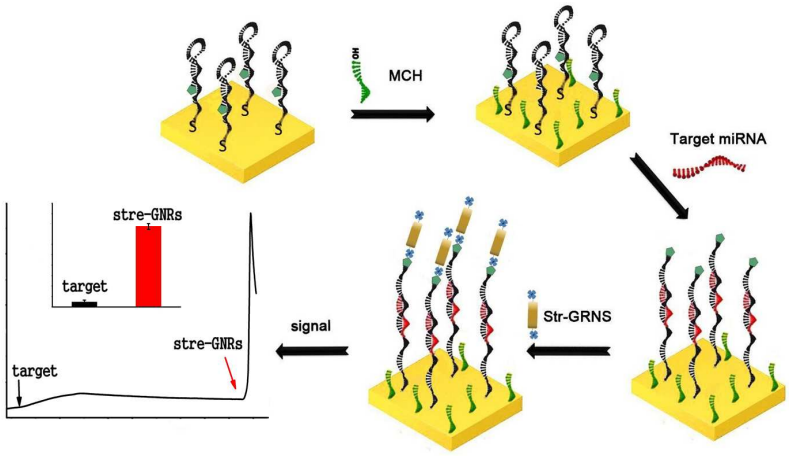

Scheme 1 Schematic illustration of the proposed method of miRNA detection based on Stre-GNRs enhanced SPR response

2. Experimental Section

2.1 Reagents and Materials.

Silver nitrate, Sodium borohydride were obtained from Sinopharm Chemical Reagent. Hydrogen tetrachloroaurate (III) hydrate ($HAuCl_4 \cdot 3H_2O$) was obtained from Shenyang Jinke reagent factory. Ascorbic acid (AA)(99%), cetyltrimethyl -ammoniumbromide (CTAB, 99%), streptavidin from Streptomyces avidinii, 6-Mercaptohexan-1-ol (MCH), Tris(2-carboxyethyl) phosphine hydrochloride (TCEP) were from Sigma-Aldrich. 1-Ethyl-(3-dimethyllaminopropyl)carbodiie hydrochlide (EDC), thioctic acid (TA) were from Alfa-Aesar. All reagents were analytical reagents. The hybrid buffer was 100 mM phosphate buffer saline (PBS, pH 7.4) containing 0.9% sodium chloride. Oligonucleotides were from Sangon, which were purified by

using high performance liquid chromatography (HPLC). All RNA sequences were from GenePharma and purified by using HPLC. Their sequences were presented in (Table 1).

Table 1 miRNA and DNA Oligonucleotides Sequence in the Experiments

Oligonucleotide Sequence	(5'-----3')
MB probe	5'-SH-TTA GCA C CGC CAA TAT TTA CGT GCT GCT A TGC TAA-biotin-3'
Complementary target	5'UAGCAGCACGUAAAUAUUGGCG3'
Single-base mismatch	5'UAGCAGCACGUAAAUAUUGCCG3'
Three bases mismatch	5'UAACAGCACGAAAAUAUUGCCG3'

Red letters, mismatched bases

2.2 Instruments.

The morphology of the GNRs and Stre-GNRs was measured with transmission electron microscope (TEM) (JEM-2010F from JEOL, 200 KV). Uv-vis absorption spectra (Uv-vis) and Infrared spectrum (IR) were record with UV-1800 spectrophotometer (Shimadzu, Japan) and Thermo Nicolet 6700 spectrometer, respectively. The ultrasonic cleaning of gold film was done in KQ3200DE numerical control ultrasonic cleaners. All the miRNA SPR experiments were performed on BI-2000 SPR sensor set-up (Biosensing Instrument Inc.)

2.3 Synthesis of GNRs.

The synthesis of GNRs was based on a seed-mediated growth method involved two steps [39]. The synthesis procedure of collaurum seeds was as follows: 19.5 mL of CTAB solution (0.1 M, 30 ^{o}C) was mixed with 0.5 mL $HAuCl_4 \cdot 3H_2O$ solution (0.01 M), and 1.2 mL of $NaBH_4$ solution (0.01M) was then added with a quick stir for 2 minutes to obtain a tawny solution. The mixture was aged at room temperature for 10

minutes. For the GNR growth, the growth solution containing 19 mL of CTAB solution (0.1 M, 30 ^{o}C) was firstly mixed with 0.16 mL of $AgNO_3$ solution (0.01 M) at 25 ^{o}C for 10 minutes, and then 1 M of $HAuCl_4 \cdot 3H_2O$ (0.01 M) was added into the mixture. AA (0.1 M) was added 10 minutes later under slight shake. Afterwards, 0.032 mL of the seed solution was added into the growth solution, and the mixture was stirred for 1 minute. Sequentially, the mixture was kept in a constant temperature bath at 28 ◦C for 17 hours to generate GNRs. Finally, the solution was centrifuged and washed at 13,000 rpm for 12 min thrice to remove the excess surfactant CTAB, and then the precipitate was suspended in water containing CTAB (5 mM) and 0.1% PEG.

2.4 Preparation of Stre-GNRs Nanoprobe.

The streptavidin was firstly modified with thioctic acids (TA) via the interaction between the carboxyl group of the thioctic acid and the amido groups of the streptavidin. Briefly, 6 mL of TA (0.0026 M) firstly activated by EDC (0.067 mg/μl) for 15 min was mixed with 8 mL of streptavidin (2×10^{-7} M), and the mixture was gently shaken at room temperature for 4 hours. The mixture was dialyzed in PBS (0.01 M, pH 7.4) at 4◦C for 3 days, and a little bit Tween-80 was added to the dialysis system to speed up dialysis (Replace the dialysis solution three times a day) to obtain TA-streptavidin.

The procedures for the functionalization of GNRs with TA-streptavidin were performed as follows: 3 ml of obtained GNRs solution was added to 6ml of TA-streptavidin (2×10^{-8} M) drop by drop, and then the solution was gently shaken for 4 hours. Finally, the solution was centrifuged at 12,000 rpm for 10 min thrice

followed by suspending the precipitate in CTAB (0.005 M, pH 3.8) with 0.1% PEG each time. The final precipitate was suspended in 300 μL CTAB (0.005M, pH 3.8) with 0.1% PEG and then kept it at 4◦C for further use.

2.5 The Fabrication of SPR Sensor.

Gold film was rinsed thoroughly by alcohol firstly then by water. Dry the film with N_2 for later use. 25 μL of biotinylated DNA probe (0.1 μM) in PBS (0.1 M, pH 7.4) containing 2 μM TCEP was dripped to the gold film. The mixture was kept at 4 ◦C overnight. Then it was washed by PBS (0.1 M, pH 7.4) to remove excess probe and dried by nitrogen. 1.45×10^{-6} M of MCH was employed to block the gold film for 1 hour. Finally, the gold film was washed by water and dried by nitrogen in order to prepare for the SPR detection.

2.6 SPR MiRNA Detection (Without Stre-GNRs Label).

After installing the gold film, the injection valve was moved to the Load mode and the mode selector valve was moved to Serial mode. Adjust the instrument by installing a syringe with deionization water as follows: the flow rate was adjusted to 50 μL /min, and then 150 μL of 1% ethanol was added to sample ring. The valve was then moved to inject and make the SPR response to be 60.0 mDeg for several times. After normalization, the syringe buffer was changed to PBS (0.1 M, pH 7.4) and the flow rate was adjusted to 8 μL /min. 150 μL of PBS (0.1 M) containing different target concentrations (0.1 nM, 1 nM, 2 nM, 10 nM, 50 nM, 100 nM) was injected into the injection port when the baseline was stable. After reacting for 10 min, the valve was moved to inject mode and then the sample was released to flow analysis module

and the SPR response values can be observed at the same time. As for the selectivity detection, the reaction condition was the same as mentioned above except the base mismatch sequences (20 nM) rather than the target was injected for detection.

2.7 GNRs-streptavidin Based SPR Detection.

The normalization steps of the experiment involved were the same as steps mentioned above. The flow rate was adjusted to 50 μl /min and PBS (0.01 M, pH 7.4) was used for baseline operation. 150 μL of PBS (0.1 M) target solution (100 pM, 50 pM, 10 pM, 5 pM, 0.1 pM) was injected into injection port when the baseline was stable. The reaction time was adjusted to 10 minutes, and then it was washed by buffer solution for 25 minutes. Afterwards, the Stre-GNRs solution (2×10^{-9}M) was injected and reacted for 5 minutes followed by washing it with buffer solution for 5 minutes. Then we can observe the SPR response values at the same time.

3. Results And Discussion

3.1 Characterization of GNRs.

It was reported that the seed-mediated GNRs synthesis had good uniform shape and size as well as single crystal structure [39]. In order to determine the GNRs morphology, we observed the GNRs and Stre-GNRs by transmission electron microscope (TEM) and analyzed their distribution, respectively. As shown in (**Figure 1A)**, the average length of GNRs was 42.1 + 1.2 nm and the width was about 14.3 + 0.9 nm. According to particle size distribution, the aspect ratio was mainly calculated about 3.5 (**Inset in Figure 1A**). The modification of TA-streptavidin enables the edge

of GNRs to become obscure (**Figure 1B**), and the aspect ratio was observed to increase to be 3.67 (**Inset in Figure 1B**), indicating the successful modification of the TA-streptavidin on the transverse terminal of the GNRs. In addition, UV-vis absorption spectra further confirmed this point. As depicted in (**Figure 1C)** (red line), GNRs had a strong longitudinal absorption peak at 761 nm and a transverse adsorption at 500 nm, indicating production of high dispersion of GNRs. TA-Streptavidin was modified on the GNRs via the carboxyl – amino interaction [40], in which case the concentration of TA-streptavidin was much higher than that of GNRs to ensure their complete integration [41], (**Figure 1C**, red line) showed that the longitudinal absorption peak of Stre-GNRs was red-shifted about 18 nm compared to the GNRs, which was induced by the change of the refractive index near the GNRs surface. In order to further confirm the functionalization of streptavidin, the Fourier Transform Infrared Spectoscopy (FT-IR) of GNRs and Stre-GNRs were investigated. As presented in（**Figure 1D**）, both of the GNRs and Stre-GNRs exhibited characteristic peak appearing at 1410 cm^{-1} assigned to the vibration peak of -CH_2- resulted from the surface CTAB. Importantly, the FTIR spectrum of Stre-GNRs displayed obvious absorption peaks corresponding to the amide bands I (1638 cm^{-1}) and II (1550 cm-1) of streptavidin, respectively, which indicated that streptavidin was successfully modified on GNRs.

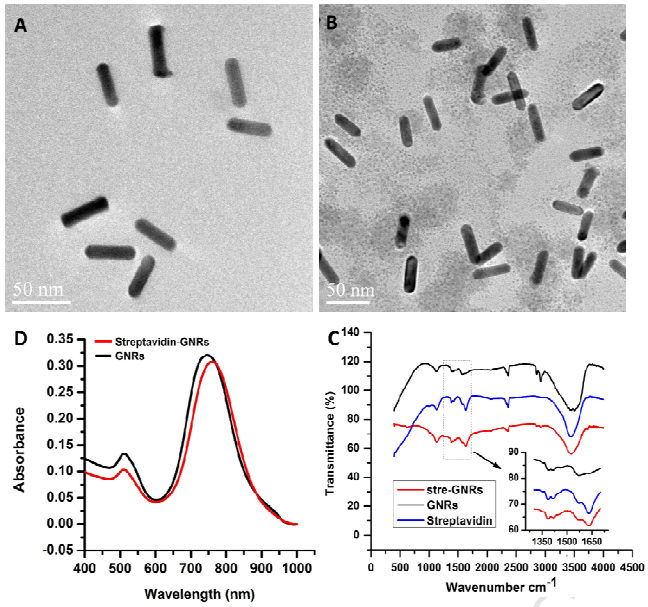

Figure 1 TEM of GNRs (A) and Stre-GNRs (B), inset (A) and (B): the particle size distribution of GNRs and Stre-GNRs; (C) The Uv-vis spectra of GNRs (black curve) and Stre-GNRs (red curve); (D) The FT-IR spectra of GNRs (black curve), Stre-GNRs (red curve) and streptavidin (blue curve) samples. Inset D: the magnified region of wavenumber from 1275 cm^{-1} to 1725 cm^{-1}.

3.2 GNRs- streptavidin amplification efficiency.

Before the detection of miRNA, we firstly studied the Stre-GNRs amplification efficiency shown in (**Figure 2)**. Arrow 1 represented the point when 5 pM target fragment was injected into the gold film which was blocked by MCH for 1 hour，while arrow 2 representing the point of the injection of 2 nM Stre-GNRs solution. A sharp increase of can be observed that after the addition of Stre-GNRs (~2190 s), because the strong interaction between biotin and streptavidin made the conjugation of Stre-GNRs on the gold film surface. It took about 5-min to archive the vertex for the whole process (inset b, Figure 2). The quick reaction was resulted from strong interaction between the biotin and streptavidin and the limited exposed biotionylated probes was 200-folds lower than the Stre-GNRs. The biotionylated probes were readily statured by the Stre-GNRs and caused prompt signal increase. It is 37.4-folds

higher than the SPR response caused by the addition of the target (**Inset in Figure 2**). For this reason, the introduction of Stre-GNRs tag increases mass and refractive index to accomplish improved detectability. Importantly, the DNA helix structure between the GNRs and gold films is about 22 bases, and the distance between of GNRs and the gold films is calculated to be 9.86 nm [42]. The electromagnetic field in LSPR of nanoparticle is strong in distance in 10 nm from the surface of the metal and decays in 10-30 nm. Therefore, the EM field of GNRs will also enhances the SPR signal due to electronic coupling of gold surface and the LSPR plasmons [43]. When the injected Stre-GNRs were completely out of flow analysis pool, Stre-GNRs were eluted from the gold film surface and the signal began to decline (~ 2790 s).

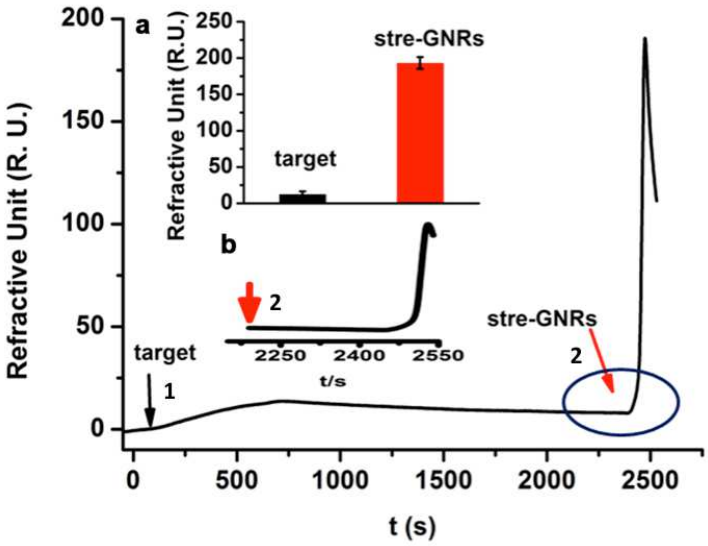

Figure 2 The SPR response of injecting 5 pM fragment (1) and 2 nM Stre-GNRs (2) after 1.45 μM MCH blocking 1 hour. PBS was used as buffer and the arrow showed the time of injecting the sample into the flow analysis pool. Inset a: the corresponding refractive unit of target and Stre-GNRs; b the magnified region of Stre-GNRs induced SPR response.

The amount of probe immobilized on the gold film will greatly influence the target capture efficiency, thus the SPR response of the biosensor. Therefore, the

concentration of the immobilized probe was optimized. Under the condition that the target concentration and Stre-GNRs was 5 pM and 2 nM, respectively, the relationship between the $\Delta\theta_2/\ \Delta\theta_1$ and the immobilized target was investigated, in which $\Delta\theta_2$ was the ratio value of refractive unit before and after adding the Stre-GNRs, and $\Delta\theta_1$ was the ratio value of refractive unit before and after adding the target. As shown in **(Figure 3)**, the $\Delta\theta_2/\ \Delta\theta_1$ increase with the increase of the immobilized probe from 5 nM to 100 nM, and the increase trend to level off when the concentration higher than 100 nM. Therefore, the concentration of the immobilized probe was selected as 100 nM in the following experiments. Meanwhile, the concentration of Stre-GNRs was also optimized under the condition that the immobilized probe and the target was fixed at 100 nM and 5 pM. It found that the $\Delta\theta_2/\ \Delta\theta_1$ increased along with the increase of Stre-GNRs ranging from 2 pM to 2 nM, and then reach to a plateau. Thus, 2 nM of Stre-GNRs was selected for the all the experiments.

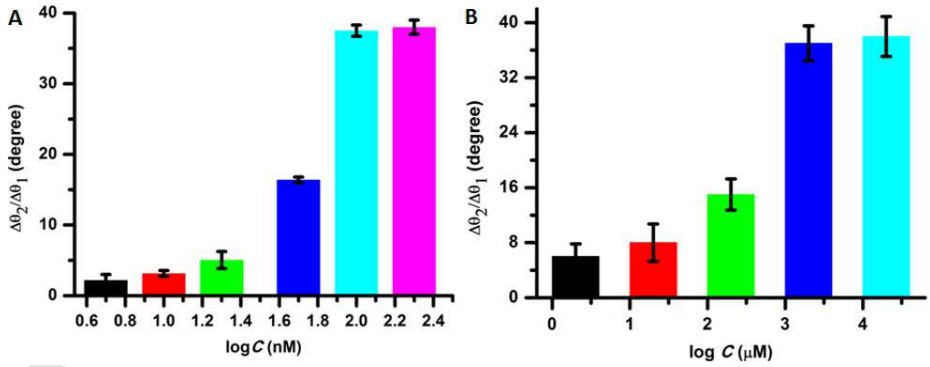

Figure 3 (A) The SPR response ratio of Stre-GNRs (2 nM) (Δθ2) to the target (5 pM) (Δθ1) at different concentrations of probes (5 nM, 10 nM, 20 nM, 50 nM, 100 nM and 200 nM). (B) the SPR response ratio of Stre-GNRs (from 2 pM-20 nM) (Δθ2) to the target (5 pM) (Δθ1) at the some concentration of probe (100 nM).

3.3 MiRNA Sensors Performance

Under the optical condition, the performances of the SPR biosensors with or without using Stre-GNRs amplification were investigated. It was found the SPR response reached a plateau after 10 minutes target injection, and no strong elution phenomenon was appeared. (**Figure 4A)** showed that the SPR response toward the target rise gradually along with the increased concentration of target. A good linear relationship was obtained between the SPR response and target concentration ranging from 0.1 to 100 nM (**Inset in Figure 4A**), and the limit of detection (LOD) was calculated to be 0.056 nm at 4-times the standard deviation of the control (free of target miRNA).

The introduction of Stre-GNRs recognized with the biotinylated DNA can drastically increase the sensitivity of sensor. (**Figure 4B)** presented the SPR response the biosensor hybridized with target at different concentration followed by introduction of Stre-GNRs (2 nM), which showed that the SPR response increase with the increase of the target, and a linear relationship between the SPR response and the target from 0.1 to 100 pM was presented (**Inset in Figure 4B**). The LOD calculated by using 4-times the standard deviation of the control (free of target miRNA) was 0.045 pM. It showed 3 magnitudes higher of the sensitivity than that without Stre-GNRs, the LOD was also superior to previous silver nanoclusters-based miRNA fluorescent detection [44] and carbon nanotube-based electrochemical detection [45]. The enhanced sensitivity might be resulted from the increase mass of the Stre-GNRs and the electronic coupling of surface and the GNRs plasmon.

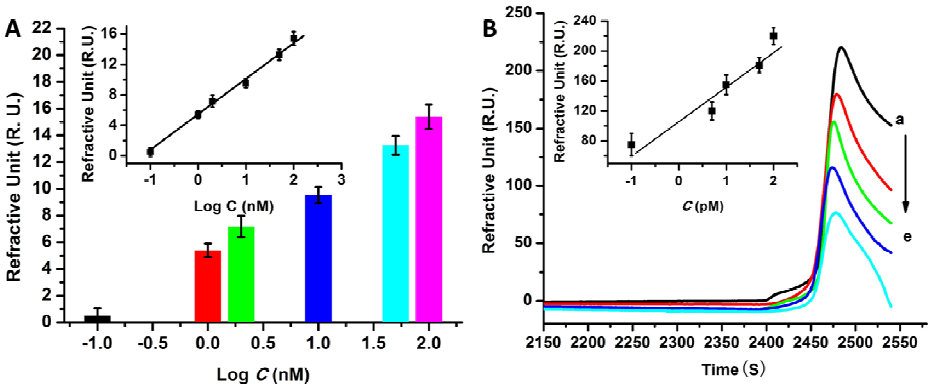

Figure 4 MiRNA detection: (A) The SPR response of the biosensor toward different target concentration (0.1 nM, 1nM, 2nM, 10 nM, 50 nM, 100 nM). RSD: 0.1-100 nM was 11%, 9.2%, 11.1%, 6.3%, 5.3% and 5.8%, respectively. (B) The SPR response of the biosensor to different miRNA concentrations (0.1 pM, 5 pM, 10 pM, 50 pM, 100 pM) followed by adding Stre-GNRs (2 nM), RSD: 0.1 pM-100 pM was 15.1%, 10%, 8.4%, 5.5% and 5%, respectively. Inset (A) and (B): Linear relationship between the refractive unit and the logarithm of the target miRNA concentration (n=4).

Compared with the linear DNA probe, MB probe possesses significant advantages in the selective detection of target due to its strong and stable sterm-loop structure and competitive dynamics. Three types of miRNA sequences including completely complementary strands, single-base mismatch chains and three bases mismatch chains in the same conditions, respectively, to explore the selectivity of the proposed assay for the target detection. As shown in **Figure 5,** the complementary target produced stronger SPR response (curve black) than the single-base mismatch sequence (curve red), while the SPR response of the three-base mismatch sequence was the lowest (green curve). The SPR response value of the single-base mismatch sequences was 63% of the complete complementary sequences, while the SPR response value of the complete complementary sequences was 2.96 times higher than the three-base mismatch sequence (**Inset in Figure 5**). The results showed that this proposed SPR biosensor had good capability to discriminate complete complementary sequences and mismatched sequences

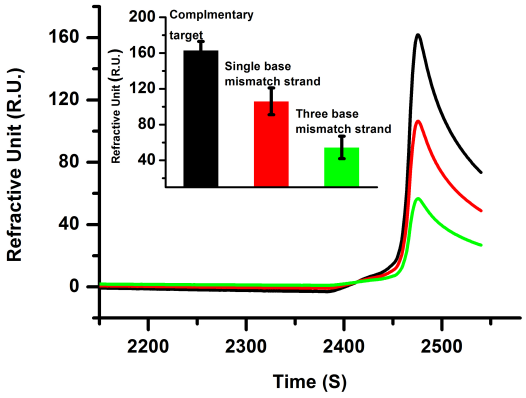

Figure 5 the SPR response the proposed sensor toward three different sequences including completely complementary, single-base mismatch and three-base mismatch sequence in the some concentration followed by using stre-GNR (2 nM) as tag. Inset: the refractive unit of different sequence (n=4). RSD: completely complementary, single-base mismatch and three-base mismatch sequence was 8.4%, 10.2% and 9.5%, respectively.

4. Conclusion

In summary, a novel SPR detection strategy by applying biotinylated thiolated molecular beacon (MB) interfacial gene probe and a strepavidinylated GNR (Stre-GNR) for the enhanced SPR response to realize rapid and sensitive miRNA detection is demonstrated. TEM, UV-vis and FT-IR were used to characterize GNRs and Stre-GNRs. It was found that the introduction of Stre-GNRs to the sensor surface led to a significantly amplified SPR signal. It was speculated that the plasmonic field extension generating from the gold film to GNRs and the mass increase of the reagent due to the GNRs has resulted in a drastic sensitivity enhancement, leading to a LOD down to pM, which was 1000-folds lower than the counterpart without Stre-GNRs. Meanwhile, the intrinsic selectivity of the MB endowed the assay with good capability for discriminate base-mismatch. These results have shown that GNRs were readily served as promising amplification labels in SPR sensing technology, providing a broad space for the development of the next generation SPR biosensor technology.

5. Author Information

*Haifeng Dong email: hfdong@ustb.edu.cn; *Xueji Zhang email: zhangxueji@ustb.edu.cn

6. Acknowledgement

The work was supported by National Natural Science Foundation of China (Grant No. 21305008, 21475008, 21275017, 51373024), the Fundamental Research Funds for the Central Universities (NO. FRF-BR-15-020A); State Key Laboratory of Analytical Chemistry for Life Science SKLACLS1401; Special Foundation for State Major Research Programe of China (NO. 2016YFC0106602).

6. References

[1] Y. Huang, J. Chen, S. Zhao, M. Shi, Z.F. Chen, H. Liang, Label-free colorimetric aptasensor based on nicking enzyme assisted signal amplification and DNAzyme amplification for highly sensitive detection of protein, Anal. Chem. 85 (2013) 4423-4430.

[2] Z.S. Peng, T.F Wu, Y.T. Li, MicroRNA-370-3p inhibits human glioma cell proliferation and induces cell cycle arrest by directly targeting β-catenin, Brain Res. 1644 (2016) 53-61.

[3] C. Su, X.P. Yang, J.Y. Lou, Geniposide reduces α-synuclein by blocking microRNA-21/lysosome-associated membrane protein 2A interaction in Parkinson disease models, Brain Res. 1644 (2016) 98-106.

[4] X.J. Ding, Y.R. Yan, S.Q. Li, Y. Zhang, W. Cheng, Q. Cheng, S.J*. Ding, Surface plasmon resonance biosensor for highly sensitive detection of microRNA based on DNA super-sandwich assemblies and streptavidin signal amplification, Anal.Chim.Acta. 874 (2015) 59-65.

[5] W. Hao, L. Yaling, Y.W. Hong, W. Jun, F.Z. Fei, Z. Pei, Label-free and enzyme-free colorimetric detection of microRNA by catalyzed hairpin assembly coupled with hybridization chain reaction, Biosens.Bioelectron. 81 (2016) 303-308.

[6)]S. Ye, Y. Wu, X. Zhai, B. Tang, Asymmetric Signal Amplification for Simultaneous SERS Detection of Multiple Cancer Markers with Significantly Different Levels, Anal.Chem. 87(16) (2015) 8242–8249.

[7] B. Lu, Y.C. Sheng, J.Q. Zhang, The altered microRNA profile in andrographolide-induced inhibition of hepatoma tumor growth, Gene. 588(2) (2016) 124-133.

[8] J. Li, Y. Dai, S. Wang, Aptamer-tagged green-and yellow-emitting fluorescent silver nanoclusters for specific tumor cell imaging, Sens. Actuators A. 232 (2016) 1-8.

[9] C.W. Cheng, P.M, Chen, Y.H. Hsieh, Foxo3a-mediated overexpression of microRNA-622 suppresses tumor metastasis by repressing hypoxia-inducible factor-1α in ERK-responsive lung cancer., Oncotarget. 6 (42) (2015) 44222-44238.

[10] W.F. Lv, J.M. Zhao, B. Situ, A target-triggered dual amplification strategy for sensitive detection of microRNA, Biosens.Bioelectron. 83 (2013) 250-255.

[11] S.J. Shi, L. Han, L. Deng, Dual drugs (microRNA-34a and paclitaxel)-loaded functional solid lipid nanoparticles for synergistic cancer cell suppression, J. Controlled Release. 194 (2014) 228-237.

[12] W. Liu, M.J. Zhu, H.X. Liu, Invading stacking primer: A trigger for high-efficiency isothermal amplification reaction with superior selectivity for detecting microRNA variants, Biosens.Bioelectron. 81 (2016) 309-316.

[13] A. Valoczi, C. Hornyik, N. Varga, J. Burgyan, S. Kauppinen, Z. Havelda, Sensitive and specific detection of microRNAs by northern blot analysis using LNA-modified oligonucleotide probes, Nucleic Acids Res. 32(22) (2014) e175.

[14] K.A. Cissell, Y. Rahimi, S. Shrestha, E.A. Hunt, S.K. Deo, Bioluminescence-based detection of microRNA, miR21 in breast cancer cells, Anal.Chem. 80(7) (2008) 2319-2325.

[15] C.F. Chen, D.A. Ridzon, A.J. Broomer, Z.H. Zhou, D.H. Lee, Real-time quantification of microRNAs by stem–loop RT–PCR, Nucleic Acids Res. 33(20) (2005) e179.

[16] Q. Zhang, F. Chen, F. Xu, Y. Zhao, C. Fan, Target-Triggered Three-Way Junction Structure and Polymerase/Nicking Enzyme Synergetic Isothermal Quadratic DNA Machine for Highly Specific, One-Step, and Rapid MicroRNA Detection at Attomolar Level, Anal.Chem. 86(16) (2014) 8098-8105.

[17] J. Chao, Z.H. Li, J. Li, Hybridization chain reaction amplification for highly sensitive fluorescence detection of DNA with dextran coated microarrays, Biosens.Bioelectron. 81 (2016) 92-96.

[18] Y. Xu, Y. Wang, S. Liu, Ultrasensitive and rapid detection of miRNA with three-way junction structure-based trigger-assisted exponential enzymatic amplification, Biosens.Bioelectron. 81 (2016) 236-241

[19] S. Hofmann, Y. Huang, P. Paulicka, Double-Stranded Ligation Assay for the Rapid Multiplex Quantification of MicroRNAs, Anal. Chem. 87 (24) (2015) 12104-12111.

[20] R. Li, F. Feng, Z.Z. Chen, Y.F. Bai, Sensitive detection of carcinoembryonic antigen using surface plasmon resonance biosensor with gold nanoparticles signal amplification, Talanta. 140 (2014) 143-149.

[21] J. Lu, H.H. Wang, S.J. Dong, Effect of Ag shapes and surface compositions on the photocatalytic performance of Ag/ZnO nanorods, J. Alloys Compd. 617 (2014) 869-876.

[22] Q. Luan, K. Zhou, H. Tan, Au-NPs enhanced SPR biosensor based on hairpin DNA without the effect of nonspecific adsorption, Biosens.Bioelectron. 26(5) (2011) 2473-2477.

[23] H.R. Jang, A.W. Wark, S.H. Baek, Ultrasensitive and ultrawide range detection of a cardiac biomarker on a surface plasmon resonance platform, Anal. Chem. 86(1) (2014) 814-819.

[24] N. Goswami, K.K. Chauhan, A. Saha, Analysis of surface plasmon resonance based bimetal coated tapered fiber optic sensor with enhanced sensitivity through radially polarized light, Opti.Commun. 379 (2016) 6-12.

[25] S. Mohseni, T.T. Moghadam, B. Dabirmanesh, Development of a label-free SPR sensor for detection of matrixmetalloproteinase-9 by antibody immobilization on carboxymethyldextran chip, Biosens.Bioelectron. 81 (2016) 510-516.

[26] T. Christopeit, T.J.O. Carlsen, R. Helland, Discovery of Novel Inhibitor Scaffolds against the Metallo-β-lactamase VIM-2 by Surface Plasmon Resonance (SPR) Based Fragment Screening, J. Med. Chem. 58 (21) (2015) 8671-8682.

[27] F. Zidane, G. Zeder-Lutz, D. Altschuh, Surface plasmon resonance analysis of the binding mechanism of pharmacological and peptidic inhibitors to human somatic angiotensin I-converting enzyme, Biochemistry. 52 (48) (2013) 8722-8731.

[28] S. Adams, J.Z. Zhang, Unique optical properties and applications of hollow gold nanospheres (HGNs), Coord. Chem. Rev. 320 (2016) 18-37.

[29] J.B. Li, P.H. Lei, S.J. Ding, Y. Zhang, J.R. Yang, Y.R*. Yan, An enzyme-free surface plasmon resonance biosensor for real-time detecting microRNA based on allosteric effect of mismatched catalytic hairpin assembly, Biosens. Bioelectron. 77 (2016) 435-441.

[30] R. Khan, J.H. Yun, K.B. Bae, Enhanced photoluminescence of ZnO nanorods via coupling with localized surface plasmon of Au nanoparticles, J. Alloys Compd. 682 (2016) 643-646.

[31] A. Karczmarczyk, S.M. Dubiak, M. Vorobii, Sensitive and rapid detection of aflatoxin M1 in milk utilizing enhanced SPR and p (HEMA) brushes, Biosens.Bioelectron. 81 (2016) 159-165.

[32] H. Yang, L.Q. He, Y.W. Hu, Surface plasmon resonance promoted photoelectrocatalyst by visible light from Au core Pd shell Pt cluster nanoparticles, Angew. Chem. Int. Ed. 54 (39) (2016) 11462-11466.

[33] M.K. Pal, M. Rashid, M. Bisht, Multiplexed magnetic nanoparticle-antibody conjugates (MNPs-ABS) based prognostic detection of ovarian cancer biomarkers, CA-125, β-2M and ApoA1 using fluorescence spectroscopy with comparison of surface plasmon resonance (SPR) analysis, Biosens.Bioelectron. 73 (2015) 146-152.

[34] S.H. Baek, A.W. Wark, H.J. Lee, Dual nanoparticle amplified surface plasmon resonance detection of thrombin at subattomolar concentrations, Anal. Chem. 86 (19) (2014) 9824-9829.

[35] X. Liu, Y. Yang, L.G. Mao, SPR quantitative analysis of direct detection of atrazine traces on Au-nanoparticles: nanoparticles size effect, Sens. Actuators. B. 218 (2015) 1-7.

[36] Y. Xiang, X.Y. Zhu, Q. Huang, Real-time monitoring of mycobacterium genomic DNA with target-primed rolling circle amplification by a Au nanoparticle-embedded SPR biosensor, Biosens.Bioelectron. 66 (2015) 512-519.

[37] S. Pinijsuwan, P. Rijiravanich, M. Somasundrum, W. Surareungchai, Sub-femtomolar electrochemical detection of DNA hybridization based on latex/gold nanoparticle-assisted signal amplification, Anal. Chem. 80 (2008) 6779-6784.

[38] P. Rijiravanich, M. Somasundrum, W. Surareungchai, Femtomolar electrochemical detection of DNA hybridization using hollow polyelectrolyte shells bearing silver nanoparticles, Anal. Chem. 80(2008) 3904-3909.

[39] N.J. Durr, T. Larson, D.K. Smith, Two-photon luminescence imaging of cancer cells using molecularly targeted gold nanorods, Nano let. 7(4) (2007) 941-945.

[40] L. Wang, Y. Zhu, L. Xu, Side‐by‐Side and End‐to‐End Gold Nanorod Assemblies for Environmental Toxin Sensing, Angew. Chem. Int. Ed. 49(32) (2010) 5472-5475.

[41] R.A. Nome, M.J. Guffey, N.F. Scherer, Plasmonic Interactions and Optical Forces between Au Bipyramidal Nanoparticle Dimers, J. Phys. Chem. A. 113(16) (2009) 4408-4415.

[42] P.S. Ho, The non-B-DNA structure of d(CA/TG)n does not differ from that of Z-DNA, Proc. Natl. Acad. Sci. USA. 91 (1994) 9549-9553.

[43] M. Li, Scott K. Cushing, N. Q. Wu, Plasmon-enhanced optical sensors: a review, Analyst, 140(2015)386-406.

[44] M. Zhang, Y.Q. Liu , C.Y. Yu, B. C. Yin, B. C. Ye, Multiplexed detection of microRNAs by tuning DNA-scaffolded silver nanoclusters. Analyst, 138(2013)4812-4817.

[45] F.Y. Li, J. Peng, J.J. Wang, H. Tang, L. Tan, Q.J. Xi, S.Z. Yao, Carbon nanotube-based label-free electrochemical biosensor for sensitive detection of miRNA-24, Biosens. Bioelectron.54 (2014)158-164

Highlight

1. A facile and sensitive microRNA (miRNA) biosensor was designed.
2. It allowed detection of miRNA with the limit of detection (LOD) down to 0.045 pM.
3. The stre-GNRs tag was readily served as promising amplification labels in SPR sensing technology.
4. It employed interfacial biotinylated thiolated DNA molecular beacon (MB) as probe and streptavidin functionalized gold nanorods (stre-GNRs) as tag for enhancing surface plasmon resonance (SPR) signal.
5. It was readily served as a powerful ultrasensitive sandwich assay for miRNA detection